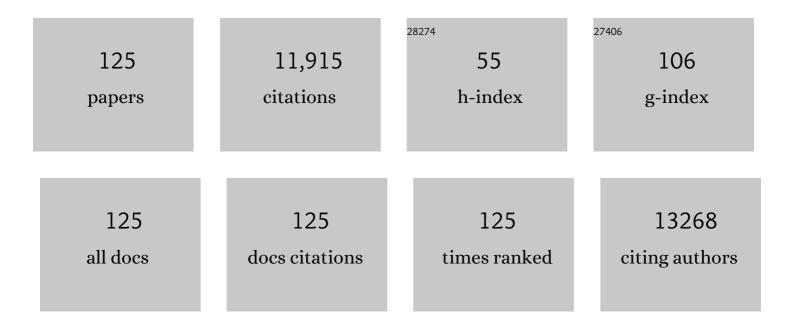
## Yusuf V Kaneti

List of Publications by Year in descending order

Source: https://exaly.com/author-pdf/8346165/publications.pdf Version: 2024-02-01



VUSUE V KANETI

#	Article	IF	CITATIONS
1	Metal–Organic Framework-Derived Nanoporous Metal Oxides toward Supercapacitor Applications: Progress and Prospects. ACS Nano, 2017, 11, 5293-5308.	14.6	988
2	Nanoarchitectured Design of Porous Materials and Nanocomposites from Metalâ€Organic Frameworks. Advanced Materials, 2017, 29, 1604898.	21.0	732
3	Nanoarchitectures for Metal–Organic Framework-Derived Nanoporous Carbons toward Supercapacitor Applications. Accounts of Chemical Research, 2016, 49, 2796-2806.	15.6	670
4	Dendriteâ€Free, Highâ€Rate, Longâ€Life Lithium Metal Batteries with a 3D Crossâ€Linked Network Polymer Electrolyte. Advanced Materials, 2017, 29, 1604460.	21.0	604
5	Metal–organic framework-derived one-dimensional porous or hollow carbon-based nanofibers for energy storage and conversion. Materials Horizons, 2018, 5, 394-407.	12.2	452
6	Strategies for Improving the Functionality of Zeolitic Imidazolate Frameworks: Tailoring Nanoarchitectures for Functional Applications. Advanced Materials, 2017, 29, 1700213.	21.0	366
7	Spontaneous Weaving of Graphitic Carbon Networks Synthesized by Pyrolysis of ZIFâ€67 Crystals. Angewandte Chemie - International Edition, 2017, 56, 8435-8440.	13.8	362
8	Fabrication of an MOF-derived heteroatom-doped Co/CoO/carbon hybrid with superior sodium storage performance for sodium-ion batteries. Journal of Materials Chemistry A, 2017, 5, 15356-15366.	10.3	317
9	Self-assembly of block copolymers towards mesoporous materials for energy storage and conversion systems. Chemical Society Reviews, 2020, 49, 4681-4736.	38.1	311
10	Core-shell motif construction: Highly graphitic nitrogen-doped porous carbon electrocatalysts using MOF-derived carbon@COF heterostructures as sacrificial templates. Chemical Engineering Journal, 2020, 396, 125154.	12.7	223
11	Solar-Powered Sustainable Water Production: State-of-the-Art Technologies for Sunlight–Energy–Water Nexus. ACS Nano, 2021, 15, 12535-12566.	14.6	220
12	General synthesis of hierarchical sheet/plate-like M-BDC (M = Cu, Mn, Ni, and Zr) metal–organic frameworks for electrochemical non-enzymatic glucose sensing. Chemical Science, 2020, 11, 3644-3655.	7.4	205
13	Unprecedented capacitive deionization performance of interconnected iron–nitrogen-doped carbon tubes in oxygenated saline water. Materials Horizons, 2020, 7, 1404-1412.	12.2	199
14	Self-assembly of nickel phosphate-based nanotubes into two-dimensional crumpled sheet-like architectures for high-performance asymmetric supercapacitors. Nano Energy, 2020, 67, 104270.	16.0	187
15	Controllable Synthesis of ZnO Nanoflakes with Exposed (101Ì0) for Enhanced Gas Sensing Performance. Journal of Physical Chemistry C, 2013, 117, 13153-13162.	3.1	176
16	Crystal plane-dependent gas-sensing properties of zinc oxide nanostructures: experimental and theoretical studies. Physical Chemistry Chemical Physics, 2014, 16, 11471-11480.	2.8	168
17	Solvothermal synthesis of ZnO-decorated α-Fe <sub>2</sub> O <sub>3</sub> nanorods with highly enhanced gas-sensing performance toward n-butanol. Journal of Materials Chemistry A, 2014, 2, 13283-13292.	10.3	164
18	Tuning the surface oxygen concentration of {111} surrounded ceria nanocrystals for enhanced photocatalytic activities. Nanoscale, 2016, 8, 378-387.	5.6	163

#	Article	IF	CITATIONS
19	Self-templated fabrication of hierarchical hollow manganese-cobalt phosphide yolk-shell spheres for enhanced oxygen evolution reaction. Chemical Engineering Journal, 2021, 405, 126580.	12.7	160
20	One-Step Synthetic Strategy of Hybrid Materials from Bimetallic Metal–Organic Frameworks for Supercapacitor Applications. ACS Applied Energy Materials, 2018, 1, 2007-2015.	5.1	159
21	Rational design and construction of nanoporous iron- and nitrogen-doped carbon electrocatalysts for oxygen reduction reaction. Journal of Materials Chemistry A, 2019, 7, 1380-1393.	10.3	159
22	Extraordinary capacitive deionization performance of highly-ordered mesoporous carbon nano-polyhedra for brackish water desalination. Environmental Science: Nano, 2019, 6, 981-989.	4.3	150
23	Self-Assembly of Two-Dimensional Bimetallic Nickel–Cobalt Phosphate Nanoplates into One-Dimensional Porous Chainlike Architecture for Efficient Oxygen Evolution Reaction. Chemistry of Materials, 2020, 32, 7005-7018.	6.7	142
24	Fabrication of highly sensitive gas sensor based on Au functionalized WO3 composite nanofibers by electrospinning. Sensors and Actuators B: Chemical, 2015, 220, 1112-1119.	7.8	138
25	MOF nanoleaves as new sacrificial templates for the fabrication of nanoporous Co–N <sub>x</sub> /C electrocatalysts for oxygen reduction. Nanoscale Horizons, 2019, 4, 1006-1013.	8.0	124
26	Multiscale structural optimization: Highly efficient hollow iron-doped metal sulfide heterostructures as bifunctional electrocatalysts for water splitting. Nano Energy, 2020, 75, 104913.	16.0	119
27	Direct fabrication of tri-metallic PtPdCu tripods with branched exteriors for the oxygen reduction reaction. Journal of Materials Chemistry A, 2018, 6, 8662-8668.	10.3	117
28	Microporous nickel phosphonate derived heteroatom doped nickel oxide and nickel phosphide: Efficient electrocatalysts for oxygen evolution reaction. Chemical Engineering Journal, 2021, 405, 126803.	12.7	112
29	Hydrothermal synthesis of ternary α-Fe2O3–ZnO–Au nanocomposites with high gas-sensing performance. Sensors and Actuators B: Chemical, 2015, 209, 889-897.	7.8	109
30	Tailorable nanoarchitecturing of bimetallic nickel–cobalt hydrogen phosphate <i>via</i> the self-weaving of nanotubes for efficient oxygen evolution. Journal of Materials Chemistry A, 2020, 8, 3035-3047.	10.3	109
31	Facile Synthesis of Nanoporous Transition Metalâ€Based Phosphates for Oxygen Evolution Reaction. ChemCatChem, 2020, 12, 2091-2096.	3.7	106
32	Borophene: Two-dimensional Boron Monolayer: Synthesis, Properties, and Potential Applications. Chemical Reviews, 2022, 122, 1000-1051.	47.7	106
33	Holey Assembly of Twoâ€Dimensional Ironâ€Doped Nickelâ€Cobalt Layered Double Hydroxide Nanosheets for Energy Conversion Application. ChemSusChem, 2020, 13, 1645-1655.	6.8	104
34	A Glucose-Assisted Hydrothermal Reaction for Directly Transforming Metal–Organic Frameworks into Hollow Carbonaceous Materials. Chemistry of Materials, 2018, 30, 4401-4408.	6.7	102
35	Mesoporous Iron Oxide Synthesized Using Poly(styrene- <i>b</i> -acrylic acid- <i>b</i> -ethylene glycol) Block Copolymer Micelles as Templates for Colorimetric and Electrochemical Detection of Glucose. ACS Applied Materials & Interfaces, 2018, 10, 1039-1049.	8.0	90
36	Advanced Functional Carbons and Their Hybrid Nanoarchitectures towards Supercapacitor Applications. ChemSusChem, 2018, 11, 3546-3558.	6.8	90

Yusuf V Kaneti

#	Article	IF	CITATIONS
37	Chemical Design of Palladiumâ€Based Nanoarchitectures for Catalytic Applications. Small, 2019, 15, e1804378.	10.0	90
38	Three-Dimensional Nanoarchitecture of Carbon Nanotube-Interwoven Metal–Organic Frameworks for Capacitive Deionization of Saline Water. ACS Sustainable Chemistry and Engineering, 2019, 7, 13949-13954.	6.7	88
39	Practical MOF Nanoarchitectonics: New Strategies for Enhancing the Processability of MOFs for Practical Applications. Langmuir, 2020, 36, 4231-4249.	3.5	86
40	Dual-Phase Transformation: Spontaneous Self-Template Surface-Patterning Strategy for Ultra-transparent VO <sub>2</sub> Solar Modulating Coatings. ACS Nano, 2017, 11, 407-415.	14.6	81
41	General template-free strategy for fabricating mesoporous two-dimensional mixed oxide nanosheets <i>via</i> self-deconstruction/reconstruction of monodispersed metal glycerate nanospheres. Journal of Materials Chemistry A, 2018, 6, 5971-5983.	10.3	81
42	Nitrogen, phosphorus co-doped eave-like hierarchical porous carbon for efficient capacitive deionization. Journal of Materials Chemistry A, 2021, 9, 12807-12817.	10.3	79
43	Li-ion and Na-ion transportation and storage properties in various sized TiO <sub>2</sub> spheres with hierarchical pores and high tap density. Journal of Materials Chemistry A, 2017, 5, 4359-4367.	10.3	78
44	A Review on Iron Oxideâ€Based Nanoarchitectures for Biomedical, Energy Storage, and Environmental Applications. Small Methods, 2019, 3, 1800512.	8.6	78
45	Assembling well-arranged covalent organic frameworks on MOF-derived graphitic carbon for remarkable formaldehyde sensing. Nanoscale, 2020, 12, 15611-15619.	5.6	78
46	Nanoarchitectonics of Biofunctionalized Metal–Organic Frameworks with Biological Macromolecules and Living Cells. Small Methods, 2019, 3, 1900213.	8.6	76
47	Nanoarchitectured peroxidase-mimetic nanozymes: mesoporous nanocrystalline α- or γ-iron oxide?. Journal of Materials Chemistry B, 2019, 7, 5412-5422.	5.8	72
48	Green synthesis of metal oxide nanostructures using naturally occurring compounds for energy, environmental, and bio-related applications. New Journal of Chemistry, 2019, 43, 15846-15856.	2.8	72
49	Experimental and theoretical studies on noble metal decorated tin oxide flower-like nanorods with high ethanol sensing performance. Sensors and Actuators B: Chemical, 2015, 219, 83-93.	7.8	70
50	Auto-programmed heteroarchitecturing: Self-assembling ordered mesoporous carbon between two-dimensional Ti3C2Tx MXene layers. Nano Energy, 2019, 65, 103991.	16.0	70
51	Nanoarchitectured Porous Conducting Polymers: From Controlled Synthesis to Advanced Applications. Advanced Materials, 2021, 33, e2007318.	21.0	68
52	Ultrathin nanosheet-assembled nickel-based metal–organic framework microflowers for supercapacitor applications. Chemical Communications, 2022, 58, 1009-1012.	4.1	68
53	Rational Design of Nanoporous MoS <sub>2</sub> /VS <sub>2</sub> Heteroarchitecture for Ultrahigh Performance Ammonia Sensors. Small, 2020, 16, e1901718.	10.0	67
54	Self-sacrificial templated synthesis of a three-dimensional hierarchical macroporous honeycomb-like ZnO/ZnCo <sub>2</sub> O <sub>4</sub> hybrid for carbon monoxide sensing. Journal of Materials Chemistry A, 2019, 7, 3415-3425.	10.3	66

#	Article	IF	CITATIONS
55	Two-dimensional mesoporous vanadium phosphate nanosheets through liquid crystal templating method toward supercapacitor application. Nano Energy, 2018, 52, 336-344.	16.0	65
56	Nanoarchitectured porous organic polymers and their environmental applications for removal of toxic metal ions. Chemical Engineering Journal, 2021, 408, 127991.	12.7	65
57	Hybrid nanoarchitecturing of hierarchical zinc oxide wool-ball-like nanostructures with multi-walled carbon nanotubes for achieving sensitive and selective detection of sulfur dioxide. Sensors and Actuators B: Chemical, 2018, 261, 241-251.	7.8	57
58	Gold nanoparticles supported on mesoporous iron oxide for enhanced CO oxidation reaction. Nanoscale, 2018, 10, 4779-4785.	5.6	54
59	Experimental and theoretical studies of gold nanoparticle decorated zinc oxide nanoflakes with exposed {1 0 <mml:math altimg="si1.gif" overflow="scroll" xmlns:mml="http://www.w3.org/1998/Math/MathML"><mml:math altimg="si1.gif" overflow="scroll" xmlns:mml="http://www.w3.org/1998/Math/MathML"><mml:math altimg="si1.gif" overflow="scroll" xmlns:mml="http://www.w3.org/1998/Math/MathML"><mml:mstyle displaystyle="true"><mml:mover accent="true"><mml:mover></mml:mover></mml:mover>&gt;&gt;</mml:mstyle></mml:math></mml:math></mml:math>	7.8	52
60	Carbon-Coated Gold Nanorods: A Facile Route to Biocompatible Materials for Photothermal Applications. ACS Applied Materials & amp; Interfaces, 2015, 7, 25658-25668.	8.0	51
61	Templateâ€Free Fabrication of Mesoporous Alumina Nanospheres Using Postâ€Synthesis Waterâ€Ethanol Treatment of Monodispersed Aluminium Clycerate Nanospheres for Molybdenum Adsorption. Small, 2018, 14, e1800474.	10.0	50
62	Mesoporous Alumina as an Effective Adsorbent for Molybdenum (Mo) toward Instant Production of Radioisotope for Medical Use. Bulletin of the Chemical Society of Japan, 2017, 90, 1174-1179.	3.2	49
63	Design and construction of polymerized-glucose coated Fe3O4 magnetic nanoparticles for delivery of aspirin. Powder Technology, 2013, 236, 157-163.	4.2	48
64	Sandwich-Structured Ordered Mesoporous Polydopamine/MXene Hybrids as High-Performance Anodes for Lithium-Ion Batteries. ACS Applied Materials & Interfaces, 2020, 12, 14993-15001.	8.0	48
65	Extracellular Vesicle Nanoarchitectonics for Novel Drug Delivery Applications. Small, 2021, 17, e2102220.	10.0	48
66	Enhanced Peroxidase Mimetic Activity of Porous Iron Oxide Nanoflakes. ChemNanoMat, 2019, 5, 506-513.	2.8	44
67	Porous FeVO4 nanorods: synthesis, characterization, and gas-sensing properties toward volatile organic compounds. Journal of Nanoparticle Research, 2013, 15, 1.	1.9	43
68	Tailored Design of Bicontinuous Gyroid Mesoporous Carbon and Nitrogenâ€Doped Carbon from Poly(ethylene oxideâ€ <i>b</i> â€caprolactone) Diblock Copolymers. Chemistry - A European Journal, 2017, 23, 13734-13741.	3.3	43
69	Crystalline Porous Organic Polymer Bearing â^'SO <sub>3</sub> H Functionality for High Proton Conductivity. ACS Sustainable Chemistry and Engineering, 2020, 8, 2423-2432.	6.7	43
70	Study on the reversible capacity loss of layered oxide cathode during low-temperature operation. Journal of Power Sources, 2017, 342, 24-30.	7.8	42
71	Molybdenum Adsorption Properties of Alumina-Embedded Mesoporous Silica for Medical Radioisotope Production. Bulletin of the Chemical Society of Japan, 2018, 91, 195-200.	3.2	42
72	Hollow Zinc Oxide Microsphere–Multiwalled Carbon Nanotube Composites for Selective Detection of Sulfur Dioxide. ACS Applied Nano Materials, 2020, 3, 8982-8996.	5.0	42

#	Article	IF	CITATIONS
73	Boronâ€Functionalized Graphene Oxideâ€Organic Frameworks for Highly Efficient CO <sub>2</sub> Capture. Chemistry - an Asian Journal, 2017, 12, 283-288.	3.3	40
74	Non-precious molybdenum nanospheres as a novel cocatalyst for full-spectrum-driven photocatalytic CO2 reforming to CH4. Journal of Hazardous Materials, 2020, 393, 122324.	12.4	39
75	Prussian blue derived iron oxide nanoparticles wrapped in graphene oxide sheets for electrochemical supercapacitors. RSC Advances, 2017, 7, 33994-33999.	3.6	36
76	Nanoarchitectonics of low-dimensional metal-organic frameworks toward photo/electrochemical CO2 reduction reactions. Journal of CO2 Utilization, 2022, 57, 101883.	6.8	36
77	Spontaneous Weaving of Graphitic Carbon Networks Synthesized by Pyrolysis of ZIFâ€67 Crystals. Angewandte Chemie, 2017, 129, 8555-8560.	2.0	33
78	Hydrothermal synthesis of sodium vanadium oxide nanorods for gas sensing application. Sensors and Actuators B: Chemical, 2014, 202, 803-809.	7.8	32
79	Enhanced Zinc Ion Storage Capability of V <sub>2</sub> O <sub>5</sub> Electrode Materials with Hollow Interior Cavities. Batteries and Supercaps, 2021, 4, 1867-1873.	4.7	31
80	Hydrogel Nanoarchitectonics: An Evolving Paradigm for Ultrasensitive Biosensing. Small, 2022, 18, .	10.0	31
81	Micron-sized Spherical Si/C Hybrids Assembled via Water/Oil System for High-Performance Lithium Ion Battery. Electrochimica Acta, 2016, 211, 982-988.	5.2	30
82	Room temperature carbon monoxide oxidation based on two-dimensional gold-loaded mesoporous iron oxide nanoflakes. Chemical Communications, 2018, 54, 8514-8517.	4.1	27
83	Mesoporous gold–silver alloy films towards amplification-free ultra-sensitive microRNA detection. Journal of Materials Chemistry B, 2020, 8, 9512-9523.	5.8	27
84	Mesoporous TiO <sub>2</sub> -based architectures as promising sensing materials towards next-generation biosensing applications. Journal of Materials Chemistry B, 2021, 9, 1189-1207.	5.8	27
85	Defect-Rich Hierarchical Porous UiO-66(Zr) for Tunable Phosphate Removal. Environmental Science & Technology, 2021, 55, 13209-13218.	10.0	27
86	Nanoarchitectured superparamagnetic iron oxide-doped mesoporous carbon nanozymes for glucose sensing. Sensors and Actuators B: Chemical, 2022, 366, 131980.	7.8	27
87	Effect of Graphene Oxide Thin Film on Growth and Electrochemical Performance of Hierarchical Zinc Sulfide Nanoweb for Supercapacitor Applications. ChemElectroChem, 2018, 5, 2636-2644.	3.4	26
88	Continuous mesoporous Pd films with tunable pore sizes through polymeric micelle-assisted assembly. Nanoscale Horizons, 2019, 4, 960-968.	8.0	26
89	Boosting capacitive performance of manganese oxide nanorods by decorating with three-dimensional crushed graphene. Nano Convergence, 2022, 9, 10.	12.1	23
90	Soft-templated synthesis of mesoporous nickel oxide using poly(styrene-block-acrylic) Tj ETQq0 0 0 rgBT /Over	lock 10 Tf 5 4.4	0 62 Td (acid

#	Article	IF	CITATIONS
91	Metal-Organic Powder Thermochemical Solid-Vapor Architectonics toward Gradient Hybrid Monolith with Combined Structure-Function Features. Matter, 2020, 3, 879-891.	10.0	22
92	Highly dispersed secondary building unit-stabilized binary metal center on a hierarchical porous carbon matrix for enhanced oxygen evolution reaction. Nanoscale, 2021, 13, 1213-1219.	5.6	22
93	Template- and etching-free fabrication of two-dimensional hollow bimetallic metal-organic framework hexagonal nanoplates for ammonia sensing. Chemical Engineering Journal, 2022, 450, 138065.	12.7	22
94	Construction of a Unique Two-Dimensional Hierarchical Carbon Architecture for Superior Lithium-Ion Storage. ACS Applied Materials & Interfaces, 2016, 8, 33399-33404.	8.0	21
95	A mesoporous tin phosphate–graphene oxide hybrid toward the oxygen reduction reaction. Chemical Communications, 2017, 53, 5721-5724.	4.1	20
96	Bilayer composites consisting of gold nanorods and titanium dioxide as highly sensitive and self-cleaning SERS substrates. Mikrochimica Acta, 2017, 184, 2805-2813.	5.0	19
97	Performance enhancement strategies for surface plasmon resonance sensors in direct glucose detection using pristine and modified UiO-66: effects of morphology, immobilization technique, and signal amplification. Journal of Materials Chemistry A, 2022, 10, 6662-6678.	10.3	19
98	Block copolymer-templated electrodeposition of mesoporous Au-Ni alloy films with tunable composition. Applied Materials Today, 2020, 18, 100526.	4.3	18
99	Deposition of gold nanoparticles on β-FeOOH nanorods for detecting melamine in aqueous solution. Journal of Colloid and Interface Science, 2012, 367, 204-212.	9.4	17
100	Hard-templated preparation of mesoporous cobalt phosphide as an oxygen evolution electrocatalyst. Electrochemistry Communications, 2019, 104, 106476.	4.7	17
101	Synthesis of platinum-decorated iron vanadate nanorods with excellent sensing performance toward n-butylamine. Sensors and Actuators B: Chemical, 2016, 236, 173-183.	7.8	16
102	Biomoleculeâ€Assisted Synthesis of Hierarchical Multilayered Boehmite and Alumina Nanosheets for Enhanced Molybdenum Adsorption. Chemistry - A European Journal, 2019, 25, 4843-4855.	3.3	16
103	Reverse micelle-mediated synthesis of plate-assembled hierarchical three-dimensional flower-like gamma-alumina particles. Microporous and Mesoporous Materials, 2021, 321, 111055.	4.4	16
104	Fabrication of highly and poorly oxidized silver oxide/silver/tin(IV) oxide nanocomposites and their comparative anti-pathogenic properties towards hazardous food pathogens. Journal of Hazardous Materials, 2021, 408, 124896.	12.4	14
105	Green Synthesis of Magnetite Nanostructures from Naturally Available Iron Sands via Sonochemical Method. Bulletin of the Chemical Society of Japan, 2018, 91, 311-317.	3.2	13
106	Confined Synthesis of Coordination Frameworks inside Double-Network Hydrogel for Fabricating Hydrogel-Based Water Pipes with High Adsorption Capacity for Cesium Ions. Bulletin of the Chemical Society of Japan, 2018, 91, 1357-1363.	3.2	12
107	Fabrication of Au functionalized TiO2 nanofibers for photocatalytic application. Journal of Nanoparticle Research, 2019, 21, 1.	1.9	11
108	Significant role of thorny surface morphology of polyaniline on adsorption of triiodide ions towards counter electrode in dye-sensitized solar cells. New Journal of Chemistry, 2021, 45, 5958-5970.	2.8	11

#	Article	IF	CITATIONS
109	Seed-mediated synthesis of dendritic platinum nanostructures with high catalytic activity for aqueous-phase hydrogenation of acetophenone. Journal of Energy Chemistry, 2015, 24, 660-668.	12.9	10
110	Gold‣oaded Nanoporous Iron Oxide Cubes Derived from Prussian Blue as Carbon Monoxide Oxidation Catalyst at Room Temperature. ChemistrySelect, 2018, 3, 13464-13469.	1.5	10
111	Single Crystal Growth of Two-Dimensional Cyano-Bridged Coordination Polymer of Co(H2O)2Ni(CN)4·4H2O Using Trisodium Citrate Dihydrate. Bulletin of the Chemical Society of Japan, 2019, 92, 1263-1267.	3.2	10
112	Mesoporous Alumina-Titania Composites with Enhanced Molybdenum Adsorption towards Medical Radioisotope Production. Bulletin of the Chemical Society of Japan, 2021, 94, 502-507.	3.2	10
113	κ-Carrageenan Gel Modified Mesoporous Gold Chronocoulometric Sensor for Ultrasensitive Detection of MicroRNA. Bulletin of the Chemical Society of Japan, 2022, 95, 198-207.	3.2	10
114	Few-layer graphitic shells networked by low temperature pyrolysis of zeolitic imidazolate frameworks. Materials Chemistry Frontiers, 2018, 2, 520-529.	5.9	9
115	Spatial-controlled etching of coordination polymers. Chinese Chemical Letters, 2021, 32, 635-641.	9.0	9
116	Selfâ€Assembly of Polymeric Micelles Made of Asymmetric Polystyreneâ€ <i>b</i> â€Polyacrylic Acidâ€ <i>b</i> â€Polyethylene Oxide for the Synthesis of Mesoporous Nickel Ferrite. European Journal of Inorganic Chemistry, 2017, 2017, 1328-1332.	2.0	8
117	Pseudocapacitive Lithium Storage of Cauliflower‣ike CoFe <sub>2</sub> O <sub>4</sub> for Lowâ€Temperature Battery Operation. Chemistry - A European Journal, 2020, 26, 13652-13658.	3.3	8
118	Tuning Wall Thicknesses in Mesoporous Silica Films for Optimization of Optical Anti-Reflective Properties. Journal of Nanoscience and Nanotechnology, 2018, 18, 100-103.	0.9	5
119	In-situ formation of Cu–Ni cyano-bridged coordination polymer on graphene oxide nanosheets and their thermal conversion. Microporous and Mesoporous Materials, 2019, 290, 109670.	4.4	5
120	Controlled Synthesis of Mesoporous Pt, Pt-Pd and Pt-Pd-Rh Nanoparticles in Aqueous Nonionic Surfactant Solution. Bulletin of the Chemical Society of Japan, 2020, 93, 455-460.	3.2	5
121	Cyano-Bridged Cu-Ni Coordination Polymer Nanoflakes and Their Thermal Conversion to Mixed Cu-Ni Oxides. Nanomaterials, 2018, 8, 968.	4.1	4
122	Role of urea on the structural, textural, and optical properties of macroemulsion-assisted synthesized holey ZnO nanosheets for photocatalytic applications. New Journal of Chemistry, 2022, 46, 9897-9908.	2.8	4
123	Micelle-Assisted Strategy for the Direct Synthesis of Large-Sized Mesoporous Platinum Catalysts by Vapor Infiltration of a Reducing Agent. Nanomaterials, 2018, 8, 841.	4.1	3
124	Fabrication and Characterization of Prussian Blue-Derived Iron Carbide-Iron Oxide Hybrid on Reduced Graphene Oxide Nanosheets. KONA Powder and Particle Journal, 2021, 38, 260-268.	1.7	2
125	Metal-Organic Powder Thermochemical Solid-Vapor Architectonics Towards Gradient Hybrid Monolith with Combined Structure-Function Features. SSRN Electronic Journal, 0, , .	0.4	0